

THEORETICAL AND EXPERIMENTAL STUDIES OF RADIATIVE AND GAS DYNAMIC PROPERTIES OF SUBSTANCES AT HIGH ENERGY DENSITY IN MATTER.

N.Yu. Orlov (1) , O.B. Denisov (1), G.A. Vergunova (2) , O.N. Rosmej (3)

1. Joint Institute for High Temperatures RAS, Izhorskaya. 13, b. 2, Moscow
2. Lebedev Physical Institute, Leninskii Prospekt, 65 Moscow
3. GSI Helmholtzzentrum für Schwerionenforschung, Plankstrasse 1, 164291 Darmstadt, Germany

Theoretical background

As known, precise measurements of physical parameters are limited for laser-produced plasma. Therefore, computer codes, which contain

1. Gas dynamics,
2. Photon transport processes,.
3. Equation of state,
4. The radiative opacity,

are used extensively to determine temperature profiles, density profiles and other plasma characteristics within the target thickness [1,2]. The radiative opacity represents an important part of this study.

1. Orzechowski, T. J., Rosen, M. D., Korblum, M. D., Porter J. L., Suter, L. J., Thissen, A. R., Wallace, R. J. (1996). The Rosseland Mean Opacity of a Mixture of Gold and Gadolinium at High Temperatures. *Phys. Rev. Lett.* **77**, pp. 3545-3548.
2. Callachan-Miller, D.& Tabak, M. (2000). Progress in target physics and design for heavy ion fusion. *Physics of Plasmas*. **7**, No. 5, pp. 2083-2091.

The density – functional theory.

In the grand canonical ensemble, the equilibrium electron density provides minimum of the grand potential

$$\Omega = Sp\{\hat{W}(\hat{H} - \mu\hat{N} + \Theta \ln \hat{W})\},$$

where the density matrix has the form

$$\hat{W} = \exp\left[-\frac{\hat{H} - \mu\hat{N}}{\Theta}\right] / Sp\left[-\frac{\hat{H} - \mu\hat{N}}{\Theta}\right], \text{ here } \Theta \text{ is the}$$

plasma temperature.

$$|\Phi_A\rangle = |n_1^A, n_2^A, \dots, n_k^A, \dots\rangle, \quad \hat{H}_A = \sum_i \hat{T}_i + \sum_{i < j} v(\vec{r}_i, \vec{r}_j)$$

$$\hat{T}_i = -\frac{1}{2}\Delta_i - \frac{Z}{r_i} + V_{ext}^A(\vec{r}_i) \quad v(\vec{r}_i, \vec{r}_j) = \frac{1}{|\vec{r}_i - \vec{r}_j|}$$

$$\hat{H}_A = \sum_{m,n} \langle m|\hat{T}|n\rangle a_m^+ a_n + \frac{1}{2} \sum_{k_1, k_2, k_3, k_4} \langle k_1 k_2 | v | k_4 k_3 \rangle a_{k_1}^+ a_{k_2}^+ a_{k_3} a_{k_4}$$

$$\Omega = \sum_A W_A E_A - \mu \sum_A W_A N_A + \Theta \sum_A W_A \ln W_A$$

The general set of self-consistent field equations that describe the state of the whole ensemble of plasma atoms and ions.

$$\hat{T}_A \Psi_i(\vec{r}_1) + V_A(\vec{r}_1) \Psi_i(\vec{r}_1) - \sum_{j \leq K} n_{Aj}^c \int \Psi_j^*(\vec{r}_2) \frac{1}{|\vec{r}_1 - \vec{r}_2|} \Psi_i(\vec{r}_2) d\vec{r}_2 \Psi_j(\vec{r}_1) = \sum_j \lambda_{ij}^A \Psi_j(\vec{r}_1),$$

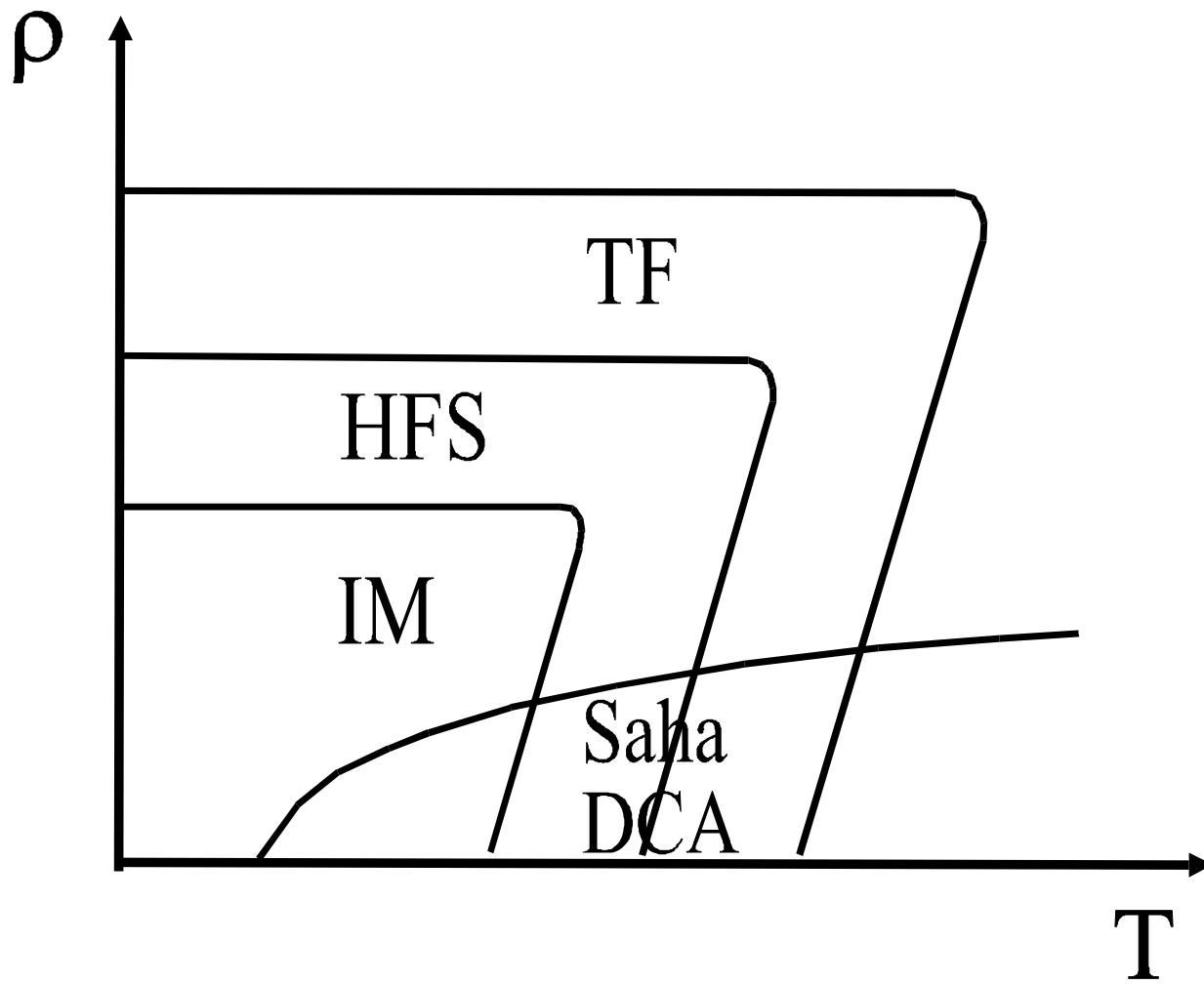
$$\bar{n}_A^f(\vec{r}, \vec{p}) = \left\{ \exp \left[\frac{1}{\Theta} \left(\frac{p^2}{2} - \frac{Z}{r} + V_A(\vec{r}) + V_{ext}^A(\vec{r}) - \mu \right) \right] + 1 \right\}^{-1}$$

- the unbound electron density in phase space

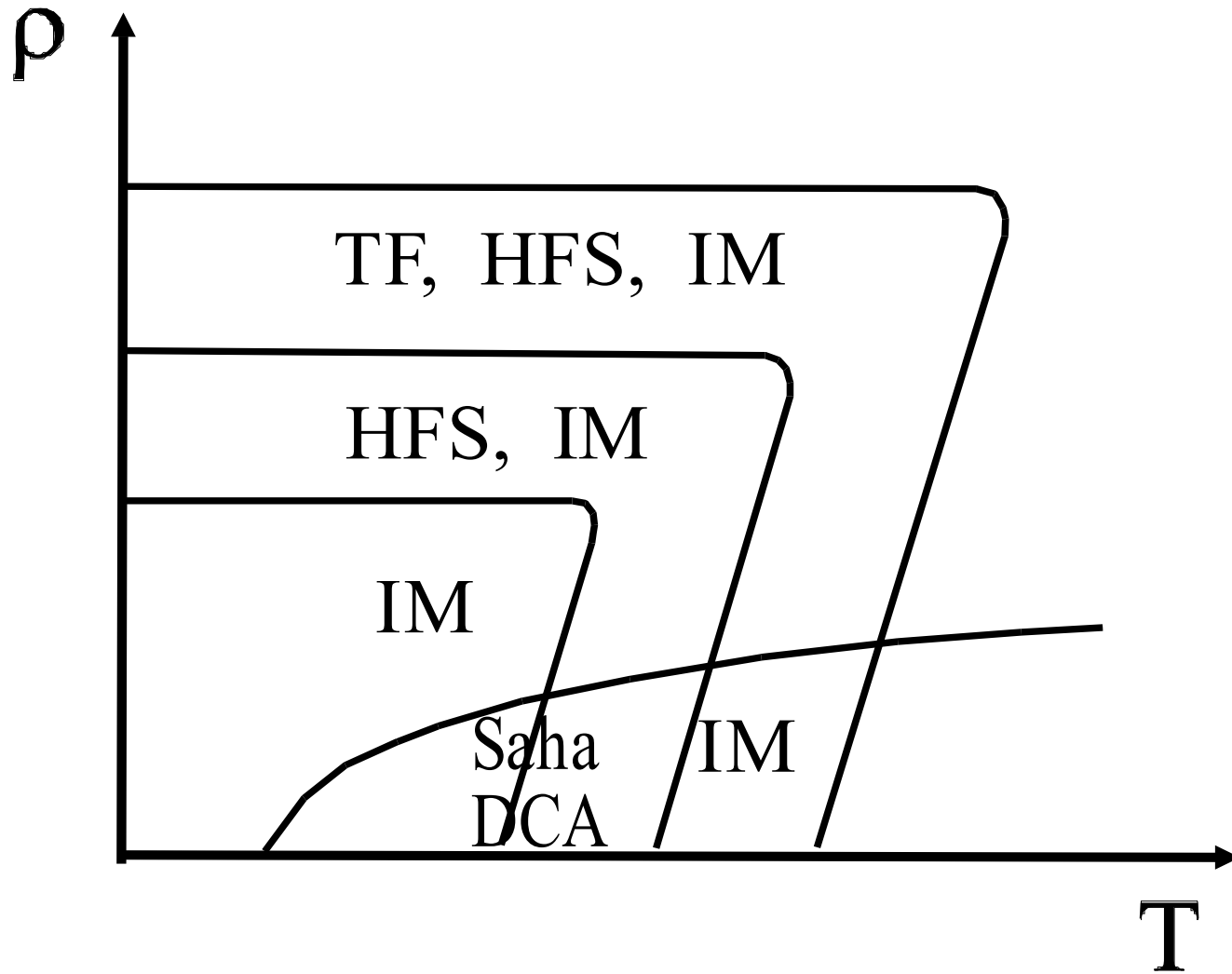
$$W_A = C g_A \exp \left\{ - \frac{E_A - \mu N_A}{\Theta} \right\},$$

$$\sum_A W_A N_A = Z.$$

Theoretical models of substances at high energy density.



Theoretical models of substances at high energy density.



Optically thick plasma.

Optically thick plasma can be produced by laser interaction with a hohlraum wall. It was shown (Orzechowski et al.) that hohlraum wall loss energy ΔE increases proportionally to the square root of the Rosseland mean free path.

$$\Delta E \propto [l_R]^{1/2} \quad (1)$$

The hohlraum wall efficiency increases with a reduction of this value. It can be achieved by decreasing the Rosseland mean free path.

Thus, an optimal chemical composition for optically thick plasmas can be achieved by minimizing the Rosseland mean free path.

Optically thin plasma.

Optically thin plasma can be produced by exploding wires in X-pinch. In this case, the outward energy flux increases inversely proportional to the Planck mean free path l_P .

$$j \propto \frac{1}{l_P} \quad (2)$$

The simple formula will be used for estimating relative radiation efficiency of different exploding wires made of two different materials A and B:

$$k = \frac{j^A}{j^B} = \frac{l_P^B}{l_P^A} \quad (3)$$

An optimal chemical composition for optically thin plasmas can be achieved by minimizing the Planck mean free path.

Results of calculations for hohlraum walls.

The spectral coefficient for x-ray absorption was calculated for gold plasma produced by laser interaction with gold hohlraum wall Au (black line). The coefficient for gold is relatively small in the energy interval $(3.5 < x < 8.5)$. The coefficient was also calculated for a composition, which is denoted as Composition 1 (red line). This composition was found using an optimization method. One can see, the interval is overlapped with spectral lines for Composition 1. It provides decreasing the Rosseland mean free path.

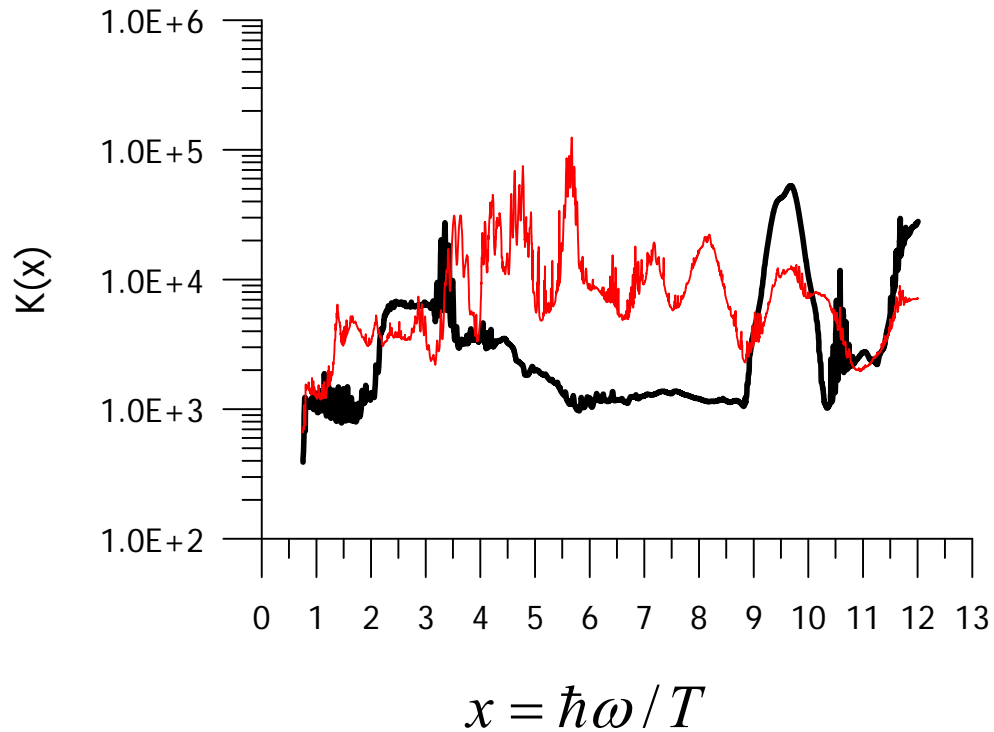


Fig.1 The spectral coefficient for X-rays absorption $K(x)$ (cm^2/g) calculated for Au (black line) and for Composition 1 (Au25.7%/W23.1%/Gd18.1%/Pr10.0%/Ba10.4%/Sb12.7%) at the temperature $T=250$ eV and the density $\tilde{\rho} = 1 \text{ g/cm}^3$.

Table 1. The hohlraum wall loss energy for different materials, compared to a Au hohlraum wall $\Delta E_{wall} / \Delta E_{Au}$ and to a AuGd hohlraum wall $\Delta E_{wall} / \Delta E_{AuGd}$.

Au		AuGd	
Material	$\frac{\Delta E_{wall}}{\Delta E_{Au}}$	Material	$\frac{\Delta E_{wall}}{\Delta E_{AuGd}}$
Au	1.00	Au/Gd(50:50)	1.00
Au:Gd	0.83	Au	1.25
U:At:W:Gd:La	0.65	Pb	1.28
U:Bi:W:Gd:La	0.65	W	1.25
U:Bi:Ta:Dy: Nd	0.63	Pb/Ta(70:30)	1.06
Th:Bi:Ta:Sm:Cs	0.68	Hg/Xe(50:50)	1.18
U:Pb:Ta:Dy:Nd	0.63	Pb/Ta/Cs(45:20:35)	1.01
U:Nb.14: Au:Ta:Dy	0.66	Pb/Hf/Xe(45:20:35)	1.00
Comp. 1	0.57	Comp. 1	0.75

1. Suter, L., Rothenberg, J., Munro, D., Vanwonderghem, B., Haan, S., & Lindl, J. (1999). Feasibility of High Yield/High Gain NIF capsules. Proceedings of International Fusion Sciences and Applications. Paris: Elsevier.

2. Callachan-Miller, D. & Tabak, M. (2000). Progress in target physics and design for heavy ion fusion. *Physics of Plasmas*. 7, No. 5, pp. 2083-2091.

Experimental and theoretical study of exploding wires in X-pinch.

The spectral coefficient for x-ray absorption was calculated for NiCr alloy (Ni80%/Cr20%) (black line) and for Alloy 188 (Cr21.72%/Ni22.92%/Fe2.24%/Co39%/ W13.93%) (red line). One can see, the energy interval is overlapped with spectral lines of Alloy 188. It leads to decreasing the Planck mean, and Alloy 188 is more efficient material. Experimental study was carried out at Cornell University to test the theoretical results. Experimental measurements were made for the total energy yield B , and the experimental and theoretical coefficients of relative efficiency can be expressed in the form:

$$k^{\text{exp}} = B^{\text{Alloy188}} / B^{\text{NiCr}} \quad k^{\text{theor}} = j^{\text{Alloy188}} / j^{\text{NiCr}}$$

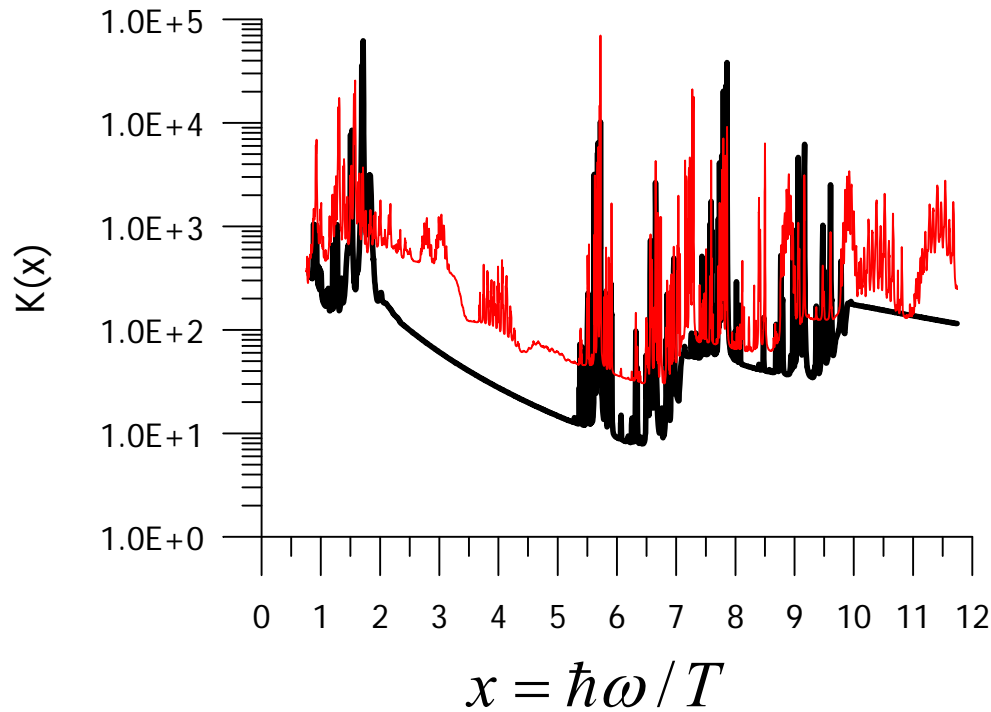


Fig. 2. The spectral coefficient for X-rays absorption $K(x)$ (cm^2/g) calculated for alloy (Ni80%/Cr20%) (black line) and for the composition Alloy 188 (Cr21.72%/Ni22.92%/Fe2.24%/Co39%/W13.93%) (red line) at the temperature $T=1$ keV and the density

$$\tilde{\rho} = \tilde{\rho}_{normal} .$$

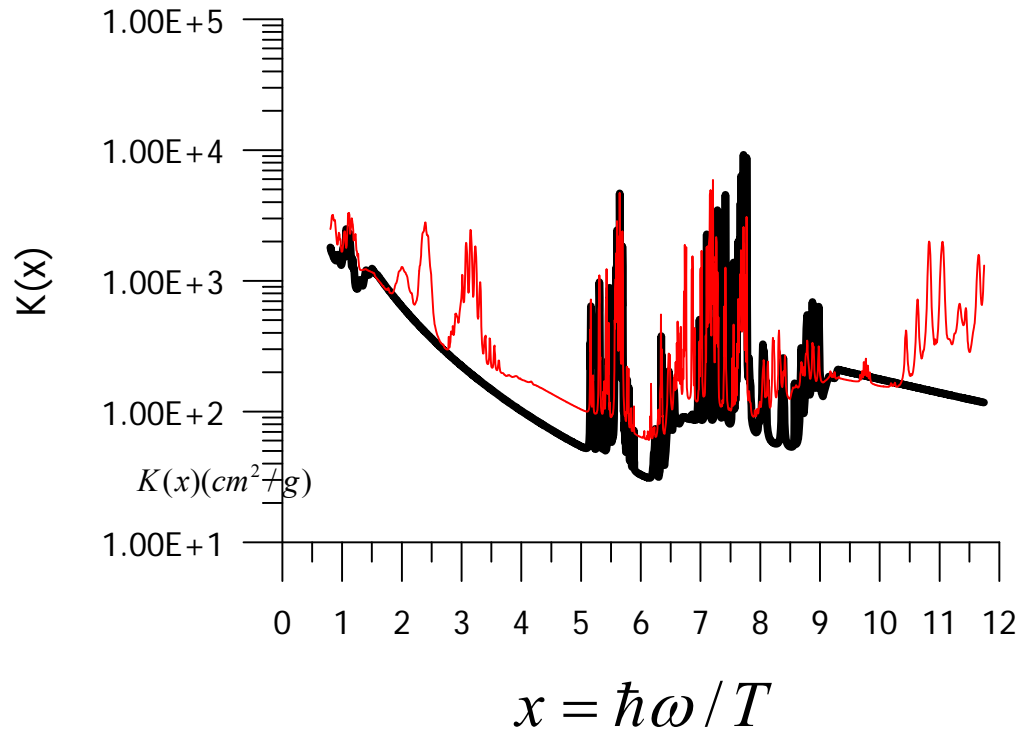


Fig. 3. The spectral coefficient of X-rays absorption calculated for NiCr (thick line) and for the composition Alloy 188 (Cr21.72%/Ni22.92%/Fe2.24%/Co39%/W13.93%) (thin line) at the temperature $T=1$ keV and the density

$$\tilde{\rho} = 10 * \tilde{\rho}_{normal}$$

Experimental and theoretical study of exploding wires in X-pinch.

The spectral coefficient for x-ray absorption was calculated for NiCr alloy (Ni80%/Cr20%) (black line) and for Alloy 188 (Cr21.72%/Ni22.92%/Fe2.24%/Co39%/ W13.93%) (red line). One can see, the energy interval is overlapped with spectral lines of Alloy 188. It leads to decreasing the Planck mean, and Alloy 188 is more efficient material. Experimental study was carried out at Cornell University to test the theoretical results. The total energy yield B was measured using two devices with different energy bands. The experimental and theoretical coefficients of relative efficiency can be expressed in the form:

$$k^{\text{exp}} = B^{\text{Alloy188}} / B^{\text{NiCr}} . \quad k^{\text{theor}} = j^{\text{Alloy188}} / j^{\text{NiCr}}$$

Table 2. Theoretical and experimental results on the relative radiation energy yield from exploding wires made of alloy (Ni80%/Cr20%) and Alloy 188 (Cr21.72%/Ni22.92%/Fe2.24%/Co39%/ W13.93%).

Experiment	Theory			
	k^{exp}	Error bar	k^{theor}	$\Delta\%$
($E > 1.5$ keV)	1.736	20%	1.84	5.6%
($2.5 < E < 5$ keV)	1.9	20%	1.84	3.2%

Experimental and theoretical study of exploding wires in X-pinch.

Thus, the experimental study confirmed the theoretical approach.

Temperature diagnostics of low Z plasma target in combined laser - heavy ion beam experiments.

The theoretical approach be used for temperature diagnostics of low Z plasma target in combined laser - heavy ion beam experiments. As known, intensity of heavy ion beam interaction with a target increases if the target is heated to plasma. The experiment needs creating a plasma target, which can keep the temperature and density during further interaction with heavy-ion beam. Indirect heating of CHO-foams with laser pulse can be used to this end.

The temperature diagnostics of CHO plasma can be based on experimental measurements of photo-absorption K-edge energies in carbon. As the temperature increases, the state of the whole ensemble of plasma atoms and ions is changed. It leads to appearance of new ions with more high ionization degree, and states with low ionization vanish. As a result, K-edge energies are considerably changed.

Comparison of the theoretical and experimental results can be used to estimate plasma temperature.

Temperature diagnostics of low Z plasma target in combined laser - heavy ion beam experiments.

Figure 3(a) presents the spectral coefficients for X-ray absorption $K(E)$ (cm^2/g) calculated for (H12 C8 O6) plasma at the density 0.002 (g/cc) and the temperature $T = 5$ eV.

Besides the absorption measurements, one can use a more convenient measurement of external source radiation, transmitted through the CHO plasma.

The green line presents the spectrum of external source radiation. If the radiation transmits through this plasma target, it creates the spectrum of transmitted radiation (red line). This line has a specific step, which coincides with K-edge position of carbon on the energy scale (Fig. 3 (b)).

Similar calculations were made for the temperature $T = 20$ eV.

The specific step position on the energy scale depends on temperature, and this fact can be used to estimate temperature of CHO plasma target.

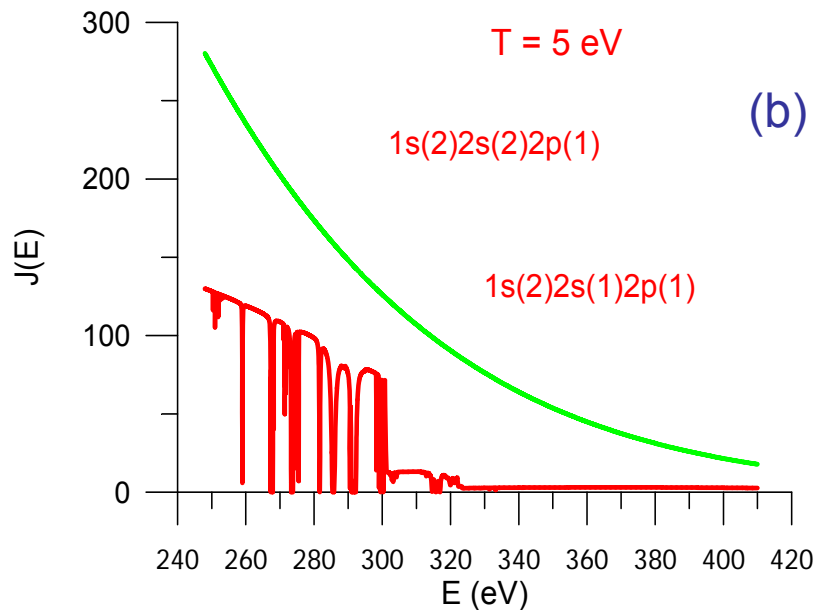
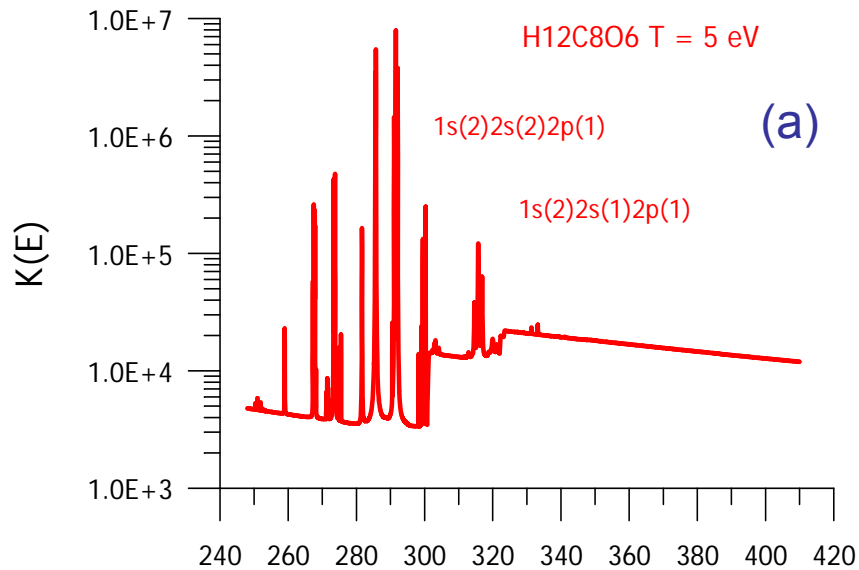


Fig.3. The spectral coefficients for X-ray absorption $K(E)$ (cm^2/g) (a) calculated for (H12 C8 O6) plasma at the density 0.002 (g/cc) and the temperature $T = 5$ eV. and the spectrum of radiation $J(E)$ ($\text{J}/\text{keV}/\text{sr}/\text{cm}^2$) (b) transmitted through the (H12 C8 O6) plasma target. The green line on the picture (b) gives the spectrum of external radiation. One can see the spectrum of transmitted radiation $J(E)$ (b) has a specific step, which coincides with K-edge position of carbon (a) on energy scale.

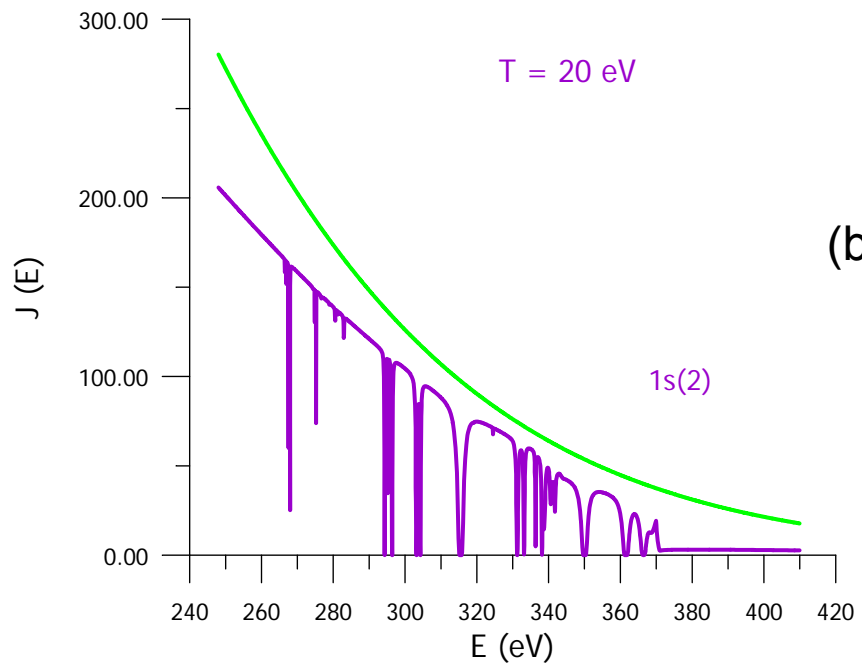
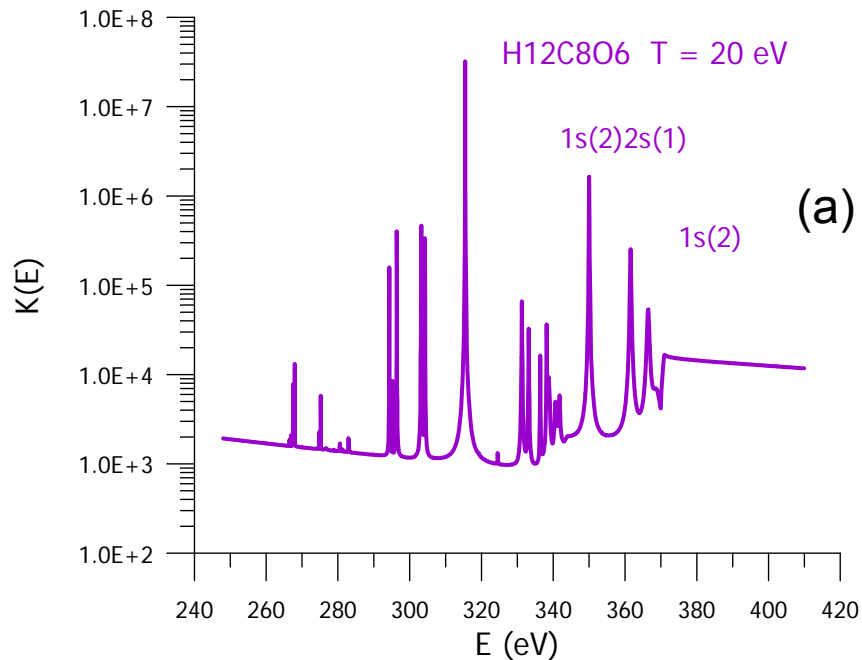


Fig. 4. The spectral coefficients for X-ray absorption $K(E)$ (cm²/g) (a) calculated for (H12 C8 O6) plasma at the density 0.002 (g/cc) and the temperature $T = 20$ eV. and the spectrum of radiation $J(E)$ (J/keV/sr/cm²) (b) transmitted through the (H12 C8 O6) plasma target. The green line on the picture (b) gives the spectrum of external radiation

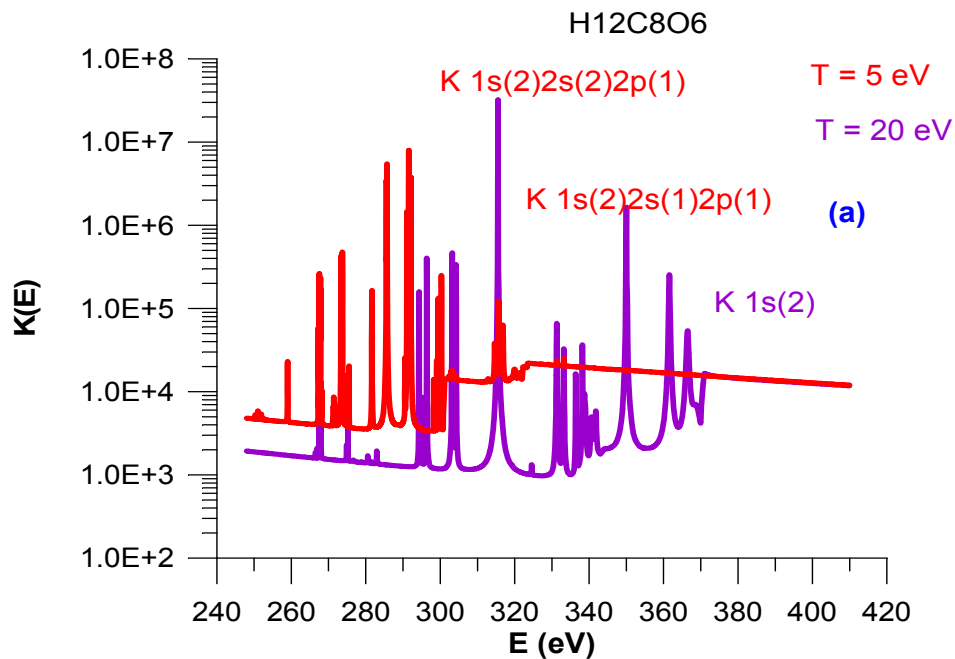


Fig. 5(a). The spectral coefficients for X-ray absorption $K(E)$ (cm^2/g) calculated for (H12 C8 O6) plasma at the density 0.002 (g/cc) and the temperature $T = 5$ eV. (red line) and $T = 20$ eV. (violet line).

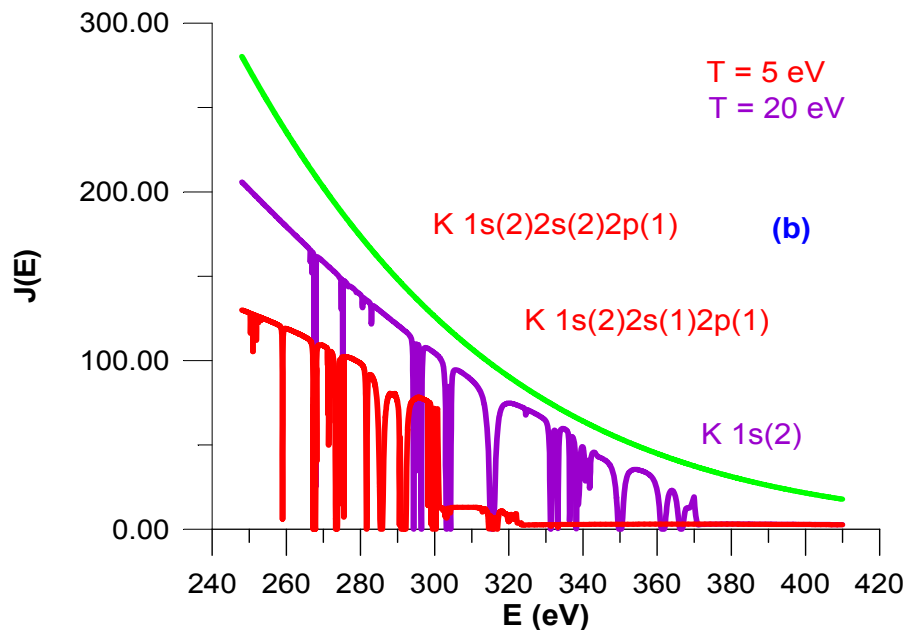


Fig. 5 (b). The spectrum of radiation $J(E)$ ($\text{J}/\text{keV}/\text{sr}/\text{cm}^2$) transmitted through the (H12 C8 O6) plasma target with the temperature $T = 5$ eV. (red line) and $T = 20$ eV. (violet line). The green line on the picture (b) gives the spectrum of external radiation.

Temperature diagnostics of low Z plasma target in combined laser - heavy ion beam experiments.

Figure 3 (a) presents the spectral coefficients for X-ray absorption $K(E)$ (cm^2/g) calculated for (H12 C8 O6) plasma at the density 0.002 (g/cc) and the temperature $T = 5$ eV.

Besides the absorption measurements, one can use a more convenient measurement of external source radiation, transmitted through the CHO plasma.

The green line presents the spectrum of external source radiation. If the radiation transmits through this plasma target, it creates the spectrum of transmitted radiation (red line). This line has a specific step, which coincides with K-edge position of carbon on the energy scale (Fig. 3 (b)).

Similar calculations were made for the temperature $T = 20$ eV.

The specific step position on the energy scale depends on temperature, and this fact can be used to estimate temperature of CHO plasma target.

Mathematical modelling of radiative and gas-dynamic processes in CHO plasma. Radiative properties of TAC and Au compositions.

Mathematical modelling of radiative and gas-dynamic processes were performed for the experiment, where hohlraum radiation transmits through the (TAC, C₁₂H₁₆O₈) plasma target during definite time interval. The share of absorbed energy in the target was calculated among other characteristics. The share was 75%, and this value agree well with experiment. The share can be increased.

A little admixture of Au can be added to TAC plasma to increase of absorbed energy in plasma target. The spectral coefficient for X-rays absorption $K(x)(\text{cm}^2/\text{g})$ was calculated for the composition (99.3% TAC and 0.7% Au) at the temperature $T = 50 \text{ eV}$. and the density 0.001 (g/cc) Fig. 6 (a). Contributions of Au (red line) and TAC (blue line) to the total coefficient were also calculated Fig.6 (b).

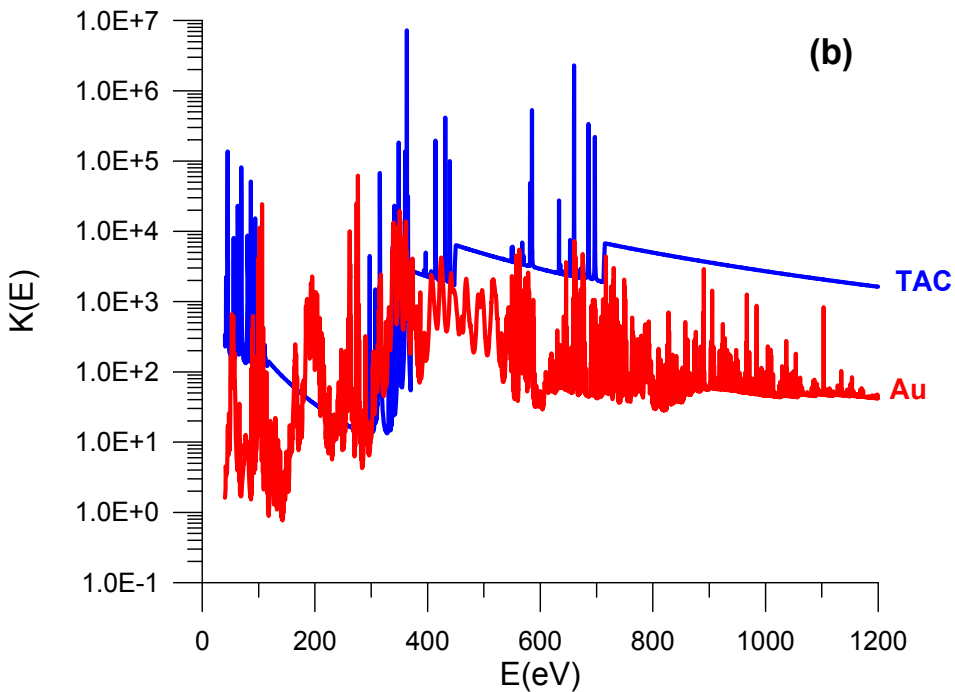
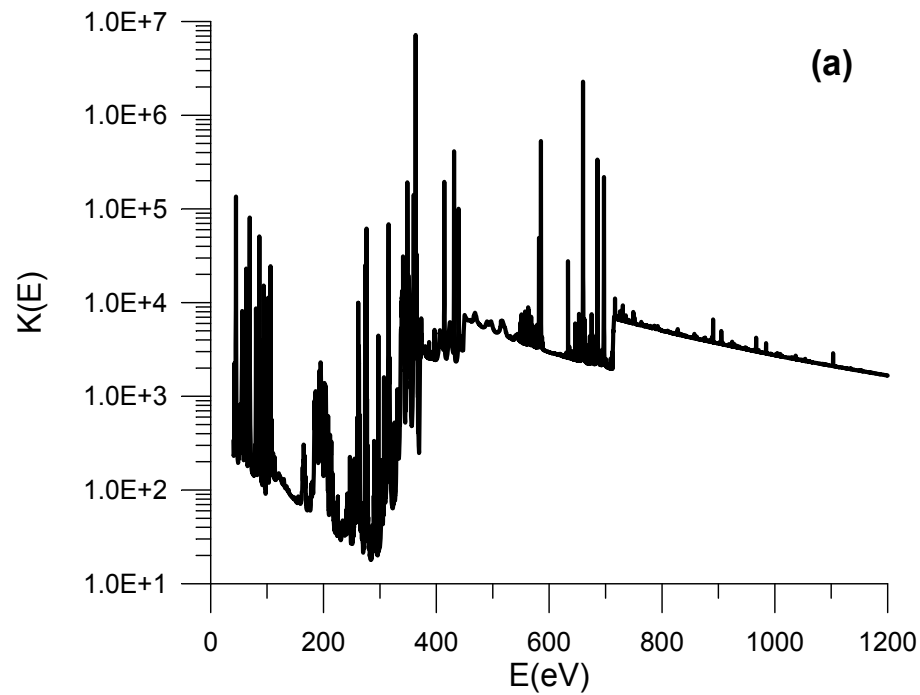


Fig. 6.

The spectral coefficient for X-rays absorption $K(x)(\text{cm}^2/\text{g})$ calculated for the composition (99.3% TAC and 0.7% Au) at the temperature $T = 50$ eV. and the density 0.001 (g/cc) (a), as well as contributions of Au (red line) and TAC (blue line) to the total coefficient (b).

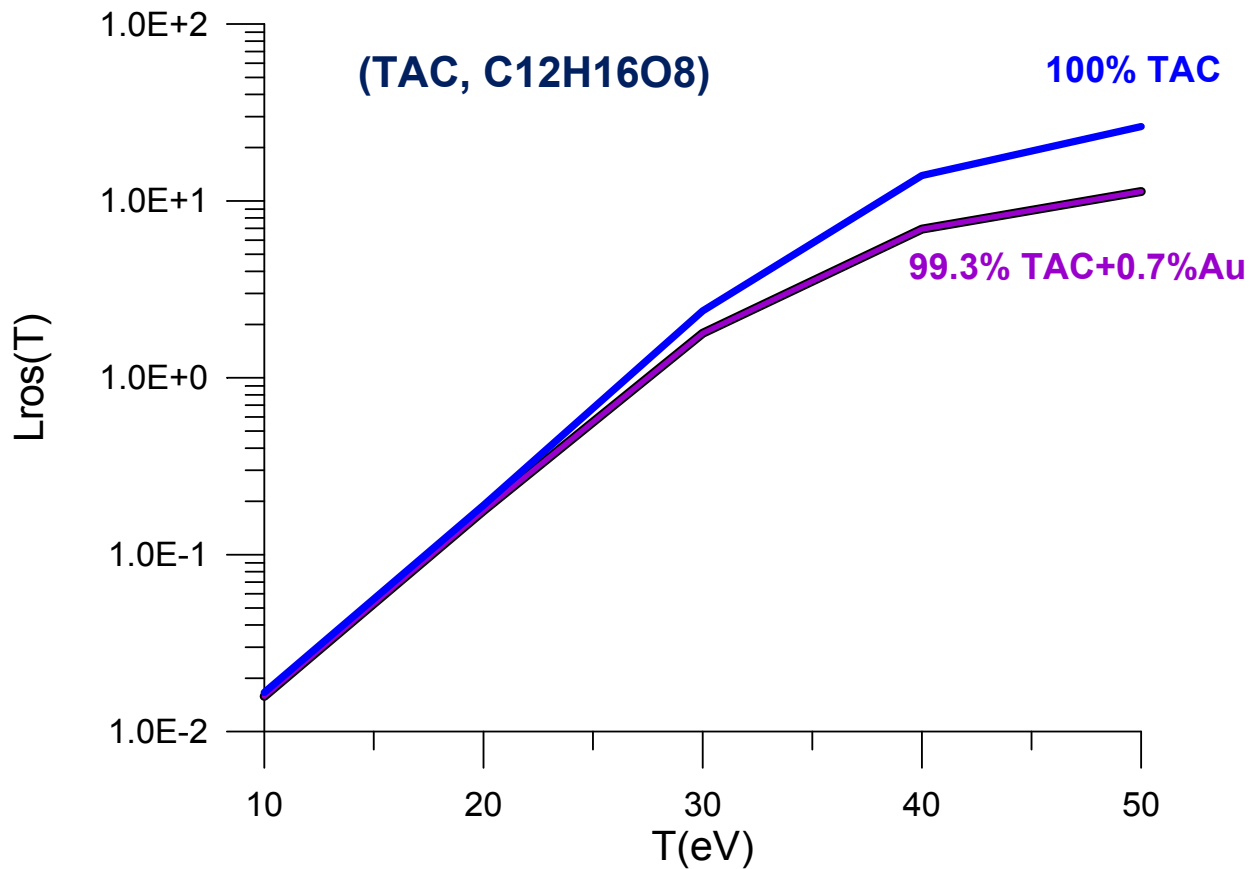
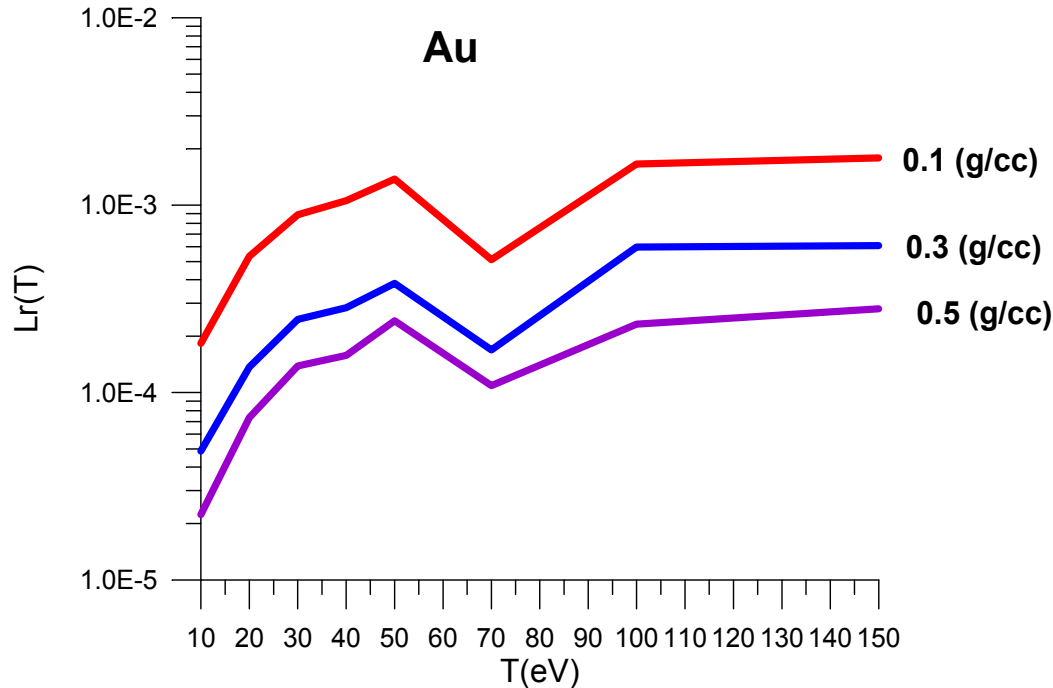


Fig. 7. The Rosseland mean free path $L_{ros}(T)$ (cm) calculated for triacetate cellulose (TAC, $C_{12}H_{16}O_8$) (blue line) and for the composition (99.3% TAC and 0.7% Au) (violet line)

Radiative properties of gold plasma



The Rosseland mean free path $L_r(T)$ (cm) calculated for gold plasma at different densities 0.1 (g/cc), 0.3 (g/cc) and 0.5 (g/cc) as a function of plasma temperature T (eV).

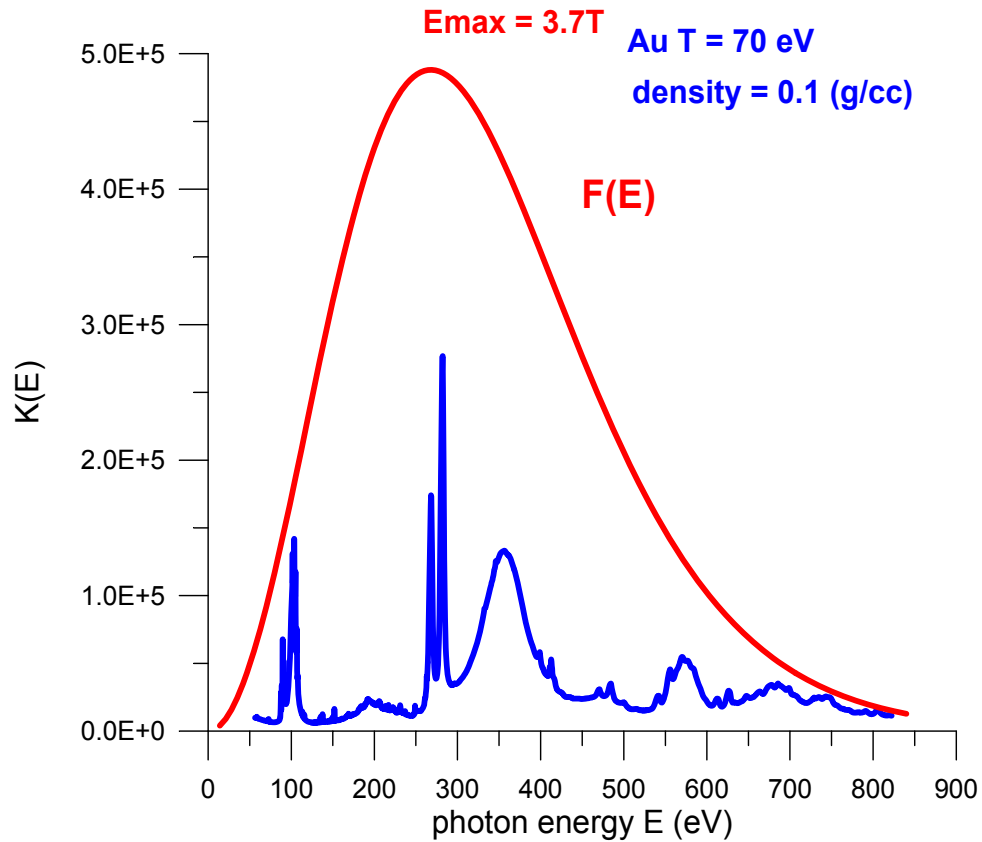
The Rosseland mean free path is calculated using the formula:

$$L_R = \frac{15}{4\pi^4} \int_0^{\infty} \frac{1}{K(E)} \frac{x^4 \exp(-x)}{(1 - \exp(-x))^2} dx$$

where $K(E)$ (1/cm) – the spectral coefficient for x-ray absorption, E – photon energy, T – plasma temperature and $x = E/T$. Function $F(x)$ has the form:

$$F(x) = \frac{x^4 \exp(-x)}{(1 - \exp(-x))^2}$$

Maximum of this function is achieved at $E_{\max} = 3.7 T$. If the temperature increases, the maximum moves along the energy scale. If E_{\max} coincides with a spectral lines group position on the energy scale, the Rosseland mean decreases.



The spectral coefficient for x-ray absorption $K(E)$ (cm^2/g) calculated for gold plasma at the temperature 70 eV. and the density 0.1 (g/cc) (blue line). The function $F(E)$ at the same temperature 70 eV. (red line)

CONCLUSIONS.

1. The Ion Model provides reliable quantum mechanical calculations of radiative opacity over a wide range of plasma temperature and density.
2. The theoretical approach can be used for temperature diagnostics of low-Z plasma and for mathematical modeling of radiative and gas-dynamic processes in plasma.